Decreasing motion artifacts in calcium-dependent fluorescence transients from the perfused mouse heart using frequency filtering

Congwu Du [a,b], Yingtian Pan [c], Guy A. MacGowan [d], Alan P. Koretsky [b,*]

[a] *Medical Department, Brookhaven National Laboratory, Upton, NY 11794, USA*
[b] *Laboratory of Functional and Molecular Imaging, NIH/NINDS, Building 10, B1D-69B, MSC 1060,*
9000 Rockville Pick, Bethesda, MD 20892, USA
[c] *Department of Biomedical Engineering, State University of New York, Stony Brook, NY 11790, USA*
[d] *Cardiovascular Institute, University of Pittsburgh, Pittsburgh, PA, USA*

Abstract

A strategy has been developed for the removal of motion artifact and noise in calcium-dependent fluorescence transients from the perfused mouse heart using frequency filtering. An analytical model indicates that the spectral removal of motion artifacts is independent of the phase shift of the motion waveform in the frequency domain, and thus to the time shift (or delay) of motion in the time domain. This is based on the "shift theorem" of Fourier analysis, which avoids erroneous correction of motion artifact when using the motion signal obtained using reflectance from the heart. Several major steps are adopted to implement this model for elimination of motion as well as detection noise from the fluorescence transient signals from the calcium-sensitive probe Rhod-2. These include (1) extracting the fluorescence calcium transient signal from the raw data by using power spectrum density (PSD) in the frequency domain by subtracting the motion recorded using the reflectance of excitation light, (2) digitally filtering out the random noise using multiple bandpass filters centralized at harmonic frequencies of the transients, and (3) extracting high frequency noise with a Gaussian Kernel filter method. The processed signal of transients acquired with excessive motion artifact is comparable to transients acquired with minimal motion obtained by immobilizing the heart against the detection window, demonstrating the usefulness of this technique.
Published by Elsevier Ltd.

Keywords: Motion artifacts; Calcium-dependent fluorescence; Perfused heart; Mouse; Frequency filtering

1. Introduction

Intracellular calcium (Ca^{2+}) is an important regulator of cardiac function [1]. Fluorescence techniques have been widely used to detect Ca^{2+} transients from isolated myocytes. Perfused or in vivo heart calcium transients have not been studied as extensively [2–7]. A major problem associated with fluorescence measurements from the intact heart is that motion causes artifactual modulation of the detected light intensity. The motion artifact arises either from a reorientation of the tissue with regard to the exciting light source and the detection optics, or from a change in the detected fluorescence intensity due to changes in tissue volume. With the beating heart, the surface moves relative to optical sensors as the contraction wave spreads across the heart. In other organs, such as the brain, changes in flow can cause the tissue to change its volume, thereby affecting the effective fluorescent volume [9].

A number of approaches have been used to suppress motion artifact. The simplest way is to physically push the heart against an optical window to immobilize the heart. However, this can cause tissue ischemia, so that real-time monitoring of the oxygenation state of the heart is usually required [5–7]. An alternative approach relies on using a reference signal obtained at a reference wavelength which can be either the reflected excitation light or a reference fluorescence emission. The fluorescence reference can be obtained from an endogenous reference fluorophore, such as NADH [10], or an added fluorophore [2,8], or a fluorescence agent that has suitable properties to act as its own reference [11]. This is applicable to those dyes with a shift property in either the excitation or emission spectrum. For example, with the calcium-sensitive dye Indo-1, the emission spectrum peak shifts from ∼480 nm with the Ca^{2+}-free form to ∼405 nm upon binding calcium. The

* Corresponding author. Tel.: +1-301-402-9659; fax: +1-301-402-0119.
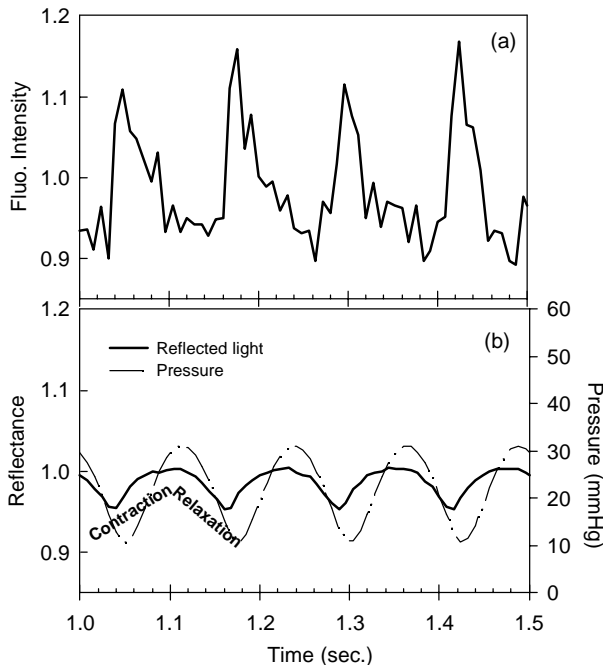*E-mail address:* koretskya@ninds.nih.gov (A.P. Koretsky).

Fig. 1. Intracellular calcium transients (a), pressure (*dotted dashed line*) and light reflectance (*solid line*) as a measure of motion (b), all of which are simultaneously obtained from the perfused mouse heart loaded with the calcium-sensitive fluorescent dye Rhod-2.

ratio between the signal and reference can be used to both suppress motion and to assess the concentration of Ca^{2+}.

In contrast to using fluorescence as a reference, using reflected excitation light provides much higher photon intensity with potentially consequent better resolution of the motion signal [10]. Most importantly, detecting reflectance can be applied to any fluorescence indicator, including non-ratiometric fluorescence dyes, such as Fluo-3 and Rhod-2. For instance, Fig. 1a shows representative intracellular calcium transients with fluorescence emission at 589 nm, which are obtained from the perfused mouse heart using the non-ratiometric calcium indicator Rhod-2. Heart motion is detected simultaneously with the transients using reflected excitation light at 524 nm as well as the pressure waveform shown in Fig. 1b. As we can see from Fig. 1b, the reflectance intensity increases with the heart's contraction and decreases with relaxation, indicating that light intensity is modulated by heart motion.

To eliminate the influence of motion artifact on the fluorescence signal, a ratio [12,13] or subtraction [10,14] between the signal and the reference is usually used. This is under the assumption that motion causes identical fluctuations in light for both the fluorescent light signal and reflected light, and thus there is no difference in the time dependence of the detected motion in the fluorescence signal and the reference. However, previous experimental evidence shows that the detected reflectance as a measure of motion may have a different time dependence to the motion artifact in the fluorescence signal. The time shift of the

motion artifact obtained by using reflected light reportedly can be as high as ~40% of a cardiac cycle period [9]. This results in an erroneous distribution in the reconstructed fluorescence signal if simply a ratio or a difference between the signal and the reflectance reference is used.

Rhod-2 has several advantages over other shorter excitation wavelength dyes, including greater tissue penetrance based on the longer excitation and emission wavelengths and a high dynamic range due to the 100-fold increase in fluorescence with Rhod-2 calcium binding. The disadvantage is that the commonly used ratio techniques to quantify relative calcium levels cannot be used as there is no shift in excitation or emission wavelengths on binding calcium. The use of absorption measurements at Rhod-2-sensitive wavelengths can be used to quantify relative levels of calcium [5,6]. There is growing interest in using Rhod-2 to measure calcium transients from the intact heart [5–7,21–24]. To decrease the influence of motion, in this study we have developed a technique to filter motion artifacts from the fluorescence signal in the frequency domain using the shift theorem of Fourier analysis which is independent of the time-shift error that may occur in the motion reference signal. The time domain signal of fluorescence Ca^{2+} transients arising from the perfused mouse heart is obtained using the calcium-sensitive, non-ratiometric fluorescent dye Rhod-2. A Fourier transform is applied, and the magnitude-mode spectrum (i.e. PSD) in the frequency domain is utilized to separate signals arising from the fluorescence transients and those resulting from motion in the frequency domain. To validate this technique, the processed signal of transients acquired with excessive motion artifact is compared with the transients acquired with minimal motion obtained by immobilizing the heart against the detection window. The result indicates that this technique can be used to minimize motion artifacts to isolate fluorescence transients due to changes in calcium concentrations.

2. Theoretical approach

The basic idea is to use the reflected excitation light as a motion reference for the calcium-dependent fluorescence in analogy to what Chance and colleagues have done for a number of years when acquiring endogenous NADH fluorescence [10]. Rather than do the correction in the time domain as has been done previously [10–14], we propose to do the correction in the frequency domain due to the fact that a magnitude Fourier transform is invariant to any time shifts between the reflected excitation and the fluorescence. The fluorescence data are thereby corrected for the appropriate frequency components of the motion. To accomplish this, it is important to properly calibrate the scaling factor or gain that properly adjusts for the amplitudes measured from the excitation light and fluorescence. In addition, we found it is important to filter noise in the frequency domain. Back Fourier transformation of the frequency domain data after correcting for motion and filtering noise recovers the

time course of the fluorescence. The details of the procedure employed are given below and in Appendices A.1–A.4.

2.1. Description of fluorescence emission and reflectance spectroscopy

To suppress motion artifact and eliminate the influence of noise on fluorescence signal, we, first of all, need to describe the components of fluorescence and reflectance spectroscopy. The intensity of the fluorescence detected at time t, is the sum of the fluorescence signal from the heart $E_{em}(t)$, background emission, such as autofluorescence from tissue $B_{em}(t)$ and the residual scattered excitation light $I_{ex}(t)$, which are modulated by system collection efficiency, or so-called system gain H_{em}. Thus, the measured intensity $S_{em}(t)$ can be described as

$$S_{em}(t) = H_{em}[E_{em}(t) + B_{em}(t) + I_{ex}(t)] \tag{1}$$

The reflectance intensity as a measure of motion artifact that is detected at the excitation wavelength can be approximately given by the following Eq. (2), as described in Appendix A.1,

$$S_{ex}(t) \approx H_{ex}[B_{ex}(t) + I_{ex}(t)] \tag{2}$$

where H_{ex} is the gain of reference channel, $B_{ex}(t)$ is the tissue background emission, and $I_{ex}(t)$ is the intensity of the reflected excitation light.

2.2. Gain calibration of reference channel

A key issue for using reflected light as a reference to monitor motion has to do with the fact that the magnitude of the gain of the reference channel (H_{ex}) is usually different to the gain of the fluorescence signal channel (H_{em}). Practically, H_{ex} is smaller than H_{em} since the reflected excitation light is much stronger than the fluorescence emission. The method we use to calibrate the gain of the reference is to use the averaged signals $\overline{S_{em}^0}$ and $\overline{S_{ex}^0}$ of the baseline in emission and in excitation that are acquired from the heart prior to loading the fluorescence dye. In Appendix A.2, we show a proportional relationship between the ratio of $\overline{S_{em}^0}$ over $\overline{S_{ex}^0}$ and the ratio of gains H_{em} over H_{ex}, i.e.

$$\frac{\overline{S_{em}^0}}{\overline{S_{ex}^0}} \approx \frac{H_{em}}{H_{ex}} \tag{3}$$

which allows us to calibrate the relative gain of the reflected light channel with respect to the emission channel, thus resulting in the motion signal obtained from reflectance channel to be normalized as $S_{ex}^{normalized}(t)$

$$S_{ex}^{normalized}(t) = \frac{\overline{S_{em}^0}}{\overline{S_{ex}^0}} S_{ex}(t) \approx \frac{H_{em}}{H_{ex}} H_{ex}[B_{ex}(t) + I_{ex}(t)]$$
$$= H_{em}[B_{ex}(t) + I_{ex}(t)] \tag{4}$$

Eq. (4) indicates an equal magnitude of gain of the reflectance channel after normalization to that of the fluorescence channel (see Eq. (1)), demonstrating that the influence of channel gain differences on the manipulation of transient signal with the reference from two detection channels is eliminated after this calibration.

2.3. Magnitude-mode frequency spectrum and the motion removal strategy

To avoid a time-shift error induced in motion artifact correction in the time domain using reflectance as the reference, a frequency domain approach is proposed to take account of the difference in the time dependence of motion artifact detected by the reflected and fluorescence light. This is based on the shift theorem of Fourier analysis which means that the magnitude-mode spectrum in frequency domain is not affected when the processed signal has a phase shift or delay in the time domain [15–17].

By definition, the magnitude-mode frequency domain spectrum of a signal, which is ordinarily referred to as the power spectrum density (PSD) of the signal, is the squared magnitude of its Fourier transform [18]. In Appendix A.3, we show that the PDS of fluorescence $|S_{em}(\omega)|^2$ and the normalized reflectance $|S_{ex}^{normalized}(\omega)|^2$ can be approximated as

$$|S_{em}(\omega)|^2 \approx H_{em}^2\{|E_{em}(\omega)|^2 + |B_{em}(\omega)|^2 + |I_{ex}(\omega)|^2\} \tag{5}$$

and

$$|S_{ex}^{normalized}(\omega)|^2 \approx H_{em}^2\{|B_{ex}(\omega)|^2 + |I_{ex}(\omega)|^2\} \tag{6}$$

Difference between $|S_{em}(\omega)|^2$ and $|S_{ex}^{normalized}(\omega)|^2$ gives

$$|S_{em}(\omega)|^2 - |S_{ex}^{normalized}(\omega)|^2 \approx H_{em}^2\{|E_{em}(\omega)|^2\} \tag{7}$$

The right-hand side of Eq. (7) remains only the power spectrum of fluorescence signal which demonstrates that the component of motion artifact, denoted as $I_{ex}(\omega)$ in the Eqs. (5) and (6), has been canceled out by calculating the difference of the PDS between the fluorescence signal and the reflected reference in the frequency domain. As Eq. (7) is independent of item of $I_{ex}(\omega)$ associated with the heart motion, the back-transformed form of Eq. (7) to time domain represents the fluorescence transient signal with the motion artifact removed.

2.4. Noise elimination

The discussion so far has assumed that the signal being measured is noise free, though practically, this is not the case as noise is always detected along with the detected signal. Fig. 2a shows two time traces of fluorescence calcium transients with low and high signal-to-noise ratios (SNR), obtained from the same mouse heart under different applied voltages on the photomultiplier detector and with a different distance from the detector to the heart. It can be noted that there is significant noise in the low SNR case. The corresponding power spectra as a function of transformed frequency for the high and low SNR cases are shown in Fig. 2b.
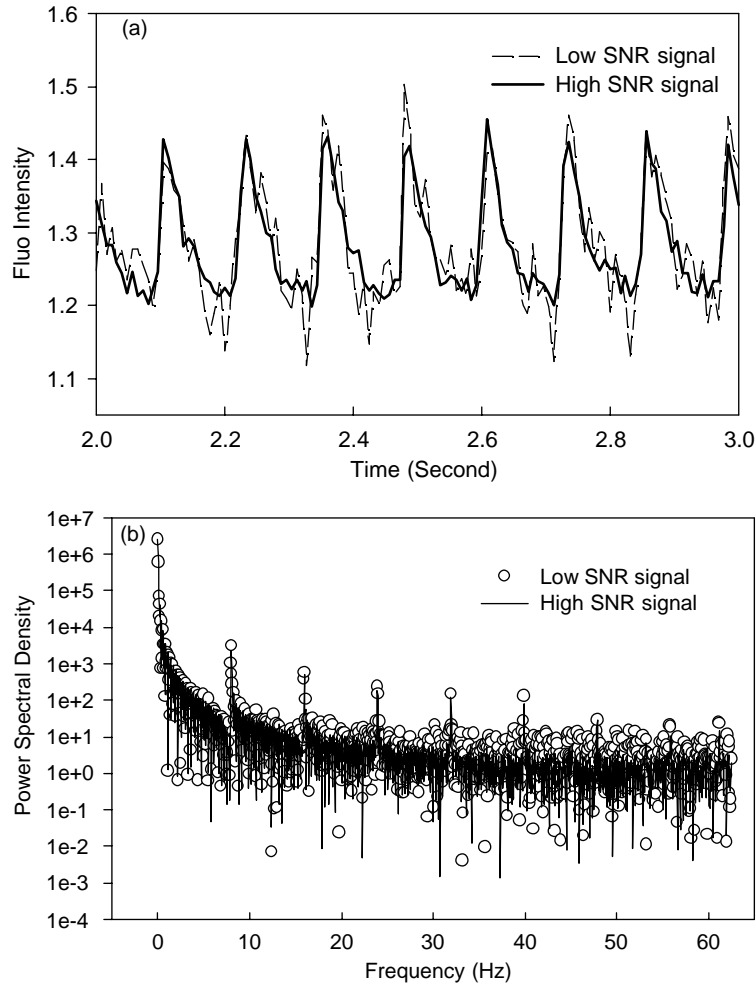
Fig. 2. Time traces of fluorescence calcium transients obtained from the mouse heart (a) and the corresponding power spectra as a function of transformed frequency (b) in cases of low and high signal-to-noise ratio (SNR). The low SNR transient signal is obtained by using the optical detector (R928, Hamamatsu) at high voltage of 760 V with a 5 cm focus distance from the heart surface, whereas the high SNR signal is at high voltage of 350 V and 1 cm focus distance.

The signal is distributed at the harmonic frequencies of 8 Hz (i.e. stimulated frequency of the heart) for both low and high SNR detection. However, the influence of noise is significantly different: it distributes relatively constantly over all frequencies, and mostly dominates at non-harmonic frequencies especially in the high frequency ranges over 50 Hz. The magnitude values of the noise between the low and high SNR signals are $\sim 10^2$ and ~ 10, respectively, which is approximately 10-fold different. On the basis of this experimental evidence, we can consider that the noise is random as a function of the transformed frequency, thus resulting in the average (over many data acquisition) noise value of zero at any given frequency. However, the corresponding spectrum

PDS of noise is non-zero due to the calculation of squaring its real and imaginary components and summing them up at correspondingly assigned frequencies. Thus, the actually measured signal $E_{em}(\omega)$ should contain an item of noise $N(\omega)$. Considering this noise item into the measurement of the fluorescence signal, i.e. the detected $E_{em}(\omega)$ becomes

$$E_{em}(\omega) = E'_{em}(\omega) + N(\omega) \tag{8}$$

where $E'_{em}(\omega)$ is noiseless signal.

To purify fluorescence signal from noise complex during PDS processing, a weight function or a filter $\phi(\omega)$ is considered as (see Appendix A.4 for derivation)

$$\begin{cases} \phi(\omega) = \dfrac{|E'_{em}(\omega)|^2}{|E'_{em}(\omega)|^2 + |N(\omega)|^2} \to 1, & \text{for } |E'_{em}(\omega)| \gg |N(\omega)| \\ \\ \phi(\omega) = \dfrac{|E'_{em}(\omega)|^2}{|E'_{em}(\omega)|^2 + |N(\omega)|^2} \to 0, & \text{for } |E'_{em}(\omega)| \ll |N(\omega)| \end{cases} \tag{9}$$
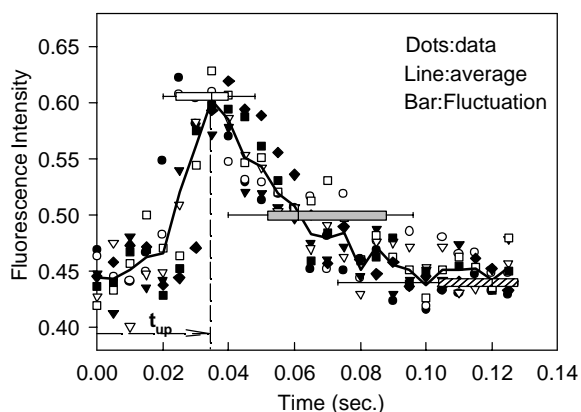
Fig. 3. Example of individual calcium-dependent transients (*circles*), the corresponding average of the transients (*solid line*) and variance in time scale and standard deviation (*bars*, $n = 40$) at peak, 50% recovery, and baseline obtained from the perfused mouse heart. The tick inside the bar represents the average value at that time point. t_{up} (=0.033 ± 0.01 s) is the mean time of the transient upstroke from base to the peak.

which means that $\phi(\omega)$ is equal to 1 (no filtering) at the frequencies where the signal predominates, but zero (completely filtered) at the frequencies where noise predominates.

Mathematically, item $E'_{em}(\omega)$ can be considered to be much greater than the item $N(\omega)$ when $|E'_{em}(\omega)| \geq 8|N(\omega)|$. Based on this, we empirically set $\phi(\omega) = 1$ when the PDS of the signal is greater than or equal to 10 times of the average noise level. It passes the signal represented at those harmonic frequencies through but eliminates the noise spectrum that is mostly scattered at those non-harmonic frequencies.

To further reduce the influence of the high frequency noise on the signal, we perform a low-pass filter using the Kernel method whose shape is Gaussian shape as a function of transformed frequency [20]. Fig. 3 is individual, mean and variance of calcium-dependent transients ($n = 40$) obtained from the perfused heart. The raw data (circles) are scattered around the average of these data (solid line) as a function of time, which indicates the fluctuations in the signal due to noise and motion. The variance of the individuals and standard deviation of the time of the maximal transient, 50% recovery from maximum and minimum transients are shown as boxes and error bars in the same graph. These indicate the variance of the transient shape due to noise, especially in the recovery portion corresponding to the maximal period of cardiac contraction. This calcium-dependent fluorescence trace characterizes a rapid upstroke of the transient during systole with a gradual decline during diastole, which indicates that the upstroke portion of the transient dominates the highest frequency of the signal in the frequency domain. The time of the transient upstroke t_{up} is defined as the time from transient base to transient peak induced by cardiac changes from diastole to systole. It is 0.033 ± 0.01 s as shown in Fig. 3, which corresponds to 30.3 Hz. So, we can set the bandwidth of the Kernel low-pass filter to ~33 Hz that cuts off high frequency noise in the calcium transient signal.

3. Materials and methods

3.1. Fluorescence transients measurements

To validate the approach proposed above, Rhod-2 fluorescence transients in perfused mouse hearts were measured along with simultaneous detection of heart motion. Techniques that have been used are similar to those described previously [5–7]. Briefly, the perfused mouse heart was stimulated at 8 Hz and placed in a water-jacketed chamber at 37 °C with an optical window on one side. To minimize the specular reflection from the air–glass–heart tissue interfaces between the optical window of the chamber and the heart, the excitation beam is focused on the heart at an incident angle of 30°, and the emission light is collected at 60° from the optical surface. Additionally, a light guide is positioned at 45° on a vertical plane to the optical window to record the heart motion waveform using the reflected excitation light from the heart during the calcium transient measurements.

After a washout period following Rhod-2 loading, an approximately fivefold increase in fluorescence above background is detected spectrofluorimetrically at 589 nm when excited at 524 nm. Calcium-dependent fluorescence transients mixed with motion artifacts and system noise are detected by a cooled photomultiplier tube (PMT R928, Hamamatsu) in the emission channel. Simultaneously, heart motion is measured by recording the reflected excitation light from the heart by using another photomultiplier tube (PMT R928, Hamamatsu) through the light guide (Oriel Co. 77568, Stratford, CT, USA). To assess the accuracy of the signal processing to eliminate motion as well as system noise from the calcium transient signals, one set of transients with minimal motion is obtained by focusing the light guide on a small area of the heart immobilized against the optical window. An excessive motion and noise artifact signal is also obtained by the more distant emission detector which collects signal from a wider area, including the freely moving portion outside the immobilized area of the heart and also from stray light. During this experiment, coronary flow, pressure, myoglobin oxygenation are monitored to ensure stability of the preparation. The signals, including Ca^{2+}-dependent fluorescence transients and the reflected excitation changes corresponding to heart motion, as well as left ventricular pressure of the heart were acquired at a sampling interval of 7.8 ms per point to provide ~16 points per cardiac cycle of 125 ms. (The heart is stimulated at 8 Hz.) As the sampling rate of 128 Hz (=1/7.8 ms) is much greater than the signal changes (8 Hz), it allows minimizing the distortion of the measured discrete data to approach the continuous signals as a function of time.

3.2. Signal processing

Fast Fourier transformation is utilized to manipulate ($N = 1024$) consecutive sampled data, which covers 64 heart beat cycles in time length, as well as Ca^{2+} fluorescence

transients. We use the power spectrum (i.e. PSD) to separate the frequency domain signals arising from the fluorescence transients and those resulting from motion.

Several major steps are adopted to implement the algorithm for elimination of motion and noise on the transient signals in the frequency domain, which includes: (1) extracting the fluorescence calcium transient signal from the raw data in the frequency domain by subtracting the motion recorded using the normalized excitation reflectance in the frequency domain, (2) digitally filtering out the random noise using multiple bandpass filters centralized at harmonic frequencies of the 8 Hz signal, and (3) reducing high frequency noise using the Kernel filter with the bandwidth of ∼33 Hz. The data are back-transformed to the time domain after processing. To assess the accuracy of this signal processing methodology, we compare the processed transient signals with the transients acquired with minimal motion as described above.
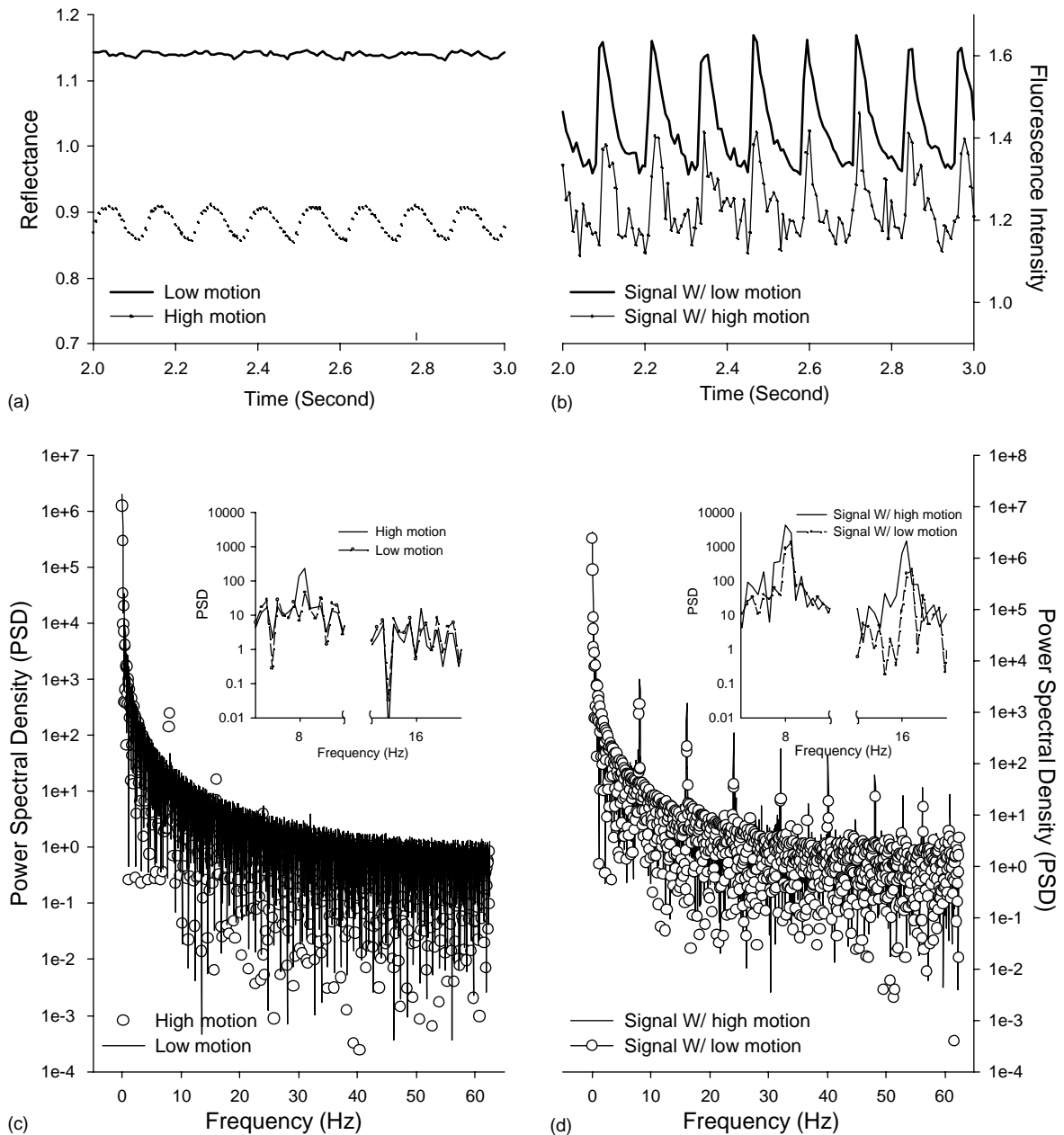

Fig. 4. Examples of motion waveform detected by using reflectance of excitation light (a), and the corresponding fluorescence transients mixed with motion (b). The power spectra as a function of the transformed frequency of the motion only (c) and transients with motion (d). The amplified view of the spectra around the frequencies of 8 and 16 Hz is shown in the inset to the figure of spectrum (c) with motion only and spectrum (d) with transients plus motion. The magnitude of motion values is estimated by using $(Motion_{peak} - Motion_{base})/(Transient_{peak} - Transient_{base})$, which are ∼6 and 20% for the low and high motion cases above, respectively.

4. Results

4.1. Spectral characterization of motion artifact in the frequency domain

Fig. 4a shows examples of motion tracings obtained from the perfused mouse heart by detecting the reflected excitation light at 524 nm. The two cases of low motion and excessive motion are shown. The corresponding fluorescence transients for the low and high motion are shown in Fig. 4b. These measurements are obtained from perfused mouse hearts under a high SNR condition. The magnitude of motion can be estimated and expressed as a percentage of fluorescence calcium transients by using the formula of $(\mathrm{Motion}_{\mathrm{peak}} - \mathrm{Motion}_{\mathrm{base}})/(\mathrm{Transient}_{\mathrm{peak}} - \mathrm{Transient}_{\mathrm{base}})$. This results in an ∼6 and 20% contribution of motion to the
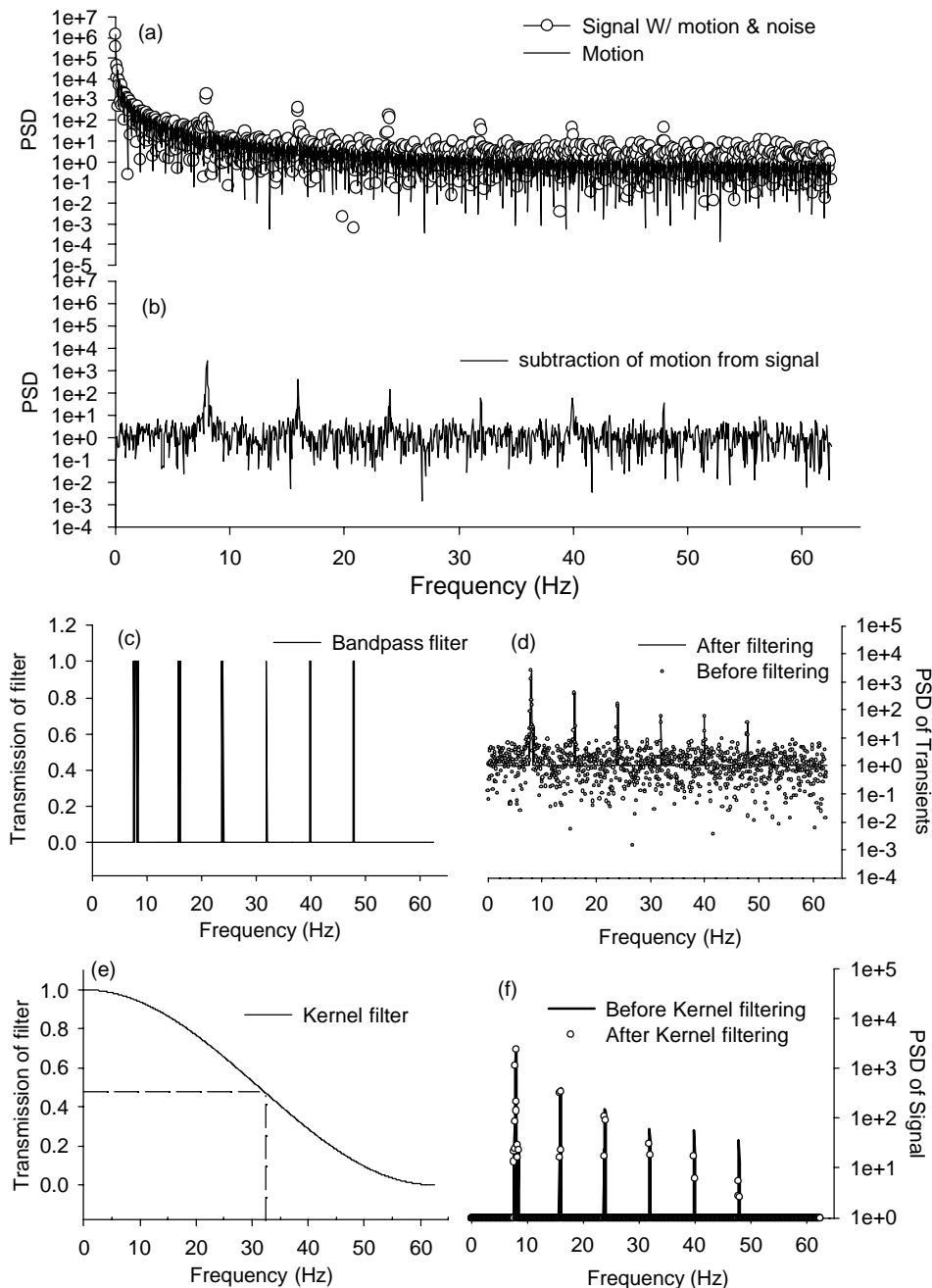

Fig. 5. Frequency filtering of fluorescence transient data to eliminate motion artifact and detection noise. (a) Transformed power spectral density of transient signal with motion and noise (*circles*) and that of motion waveform obtained simultaneously from the heart. (b) Subtraction of motion from the transient signal. (c) Bandpass filters designed according to Eq. (A.14). (d) Comparison of the transient spectra before (*dots*) and after (*solid line*) bandpass filtering. (e) Kernel filtering with a bandwidth of 33 Hz (*dashed line*) designed according to the characterization of the transient patterns shown in Fig. 3 above. (f) Comparison of the transient spectra before (*solid line*) and after (*circles*) Kernel filtering.

fluorescence transients for the low and high motion cases, respectively. The influence of these motion states on the calcium transient signals can be seen from the shape distortion of transients with 20% motion artifacts compared to that of 6%, as shown in Fig. 4b. For comparison, the PSDs of the motion only (reflected excitation light) and the transients mixed with motion artifacts (fluorescence emission) as a function of frequency are shown in Fig. 4c and d, respectively. Interestingly, the spectral bands of motion are located at the first three harmonic frequencies of 8 Hz (a stimulated frequency of the heart), i.e. 8, 16, and 24 Hz. The amplitude of PSD of the fluorescence transients with the motion artifact of 20% is greater than that of the example of motion at 6% at the harmonic frequencies of 8 Hz as shown in Fig. 4d, thus indicating that the measured spectrum intensity is a summation of the signal and the motion components, which agrees with the prediction of the above Eq. (1). In addition to spectral density at 8, 16, and 24 Hz, the calcium transient spectrum has peaks located at the other harmonic frequencies of 8 Hz, such as 32 Hz, etc. The width of these peaks tend to be narrower for the motion than for the transients plus motion as shown in the inset graphics in Fig. 4c and d. On the other hand, the spectral intensity beyond the harmonic frequencies is similar between these two exam-

ples, indicating a comparable noise level of these two measurements and that the fluorescence emission channel and reflected light channel were properly normalized.

4.2. Removal of motion artifacts and elimination of noise influence

Fig. 5 demonstrates the process of removing motion artifact for representative experimental data of fluorescence transients obtained from the perfused mouse heart. After Fourier transformation, the power spectrum of the transient signal can be obtained by calculating the summation of the squares of the real and imaginary components at each frequency. Fig. 5a shows the power spectrum of the transient signal mixed with motion and noise as a function of the transform frequency, as well as the power spectrum of motion obtained simultaneously from the same heart using the reflected excitation light. The spectrum of the subtraction of motion from the transient signal is shown in Fig. 5b, which removes the influence of motion on the signal in the power spectrum as described in the above Eq. (7). It should be pointed out that, as noise is random as a function of time and frequency, it results in an uncorrelated power magnitude of the noise at any frequency between the signal and
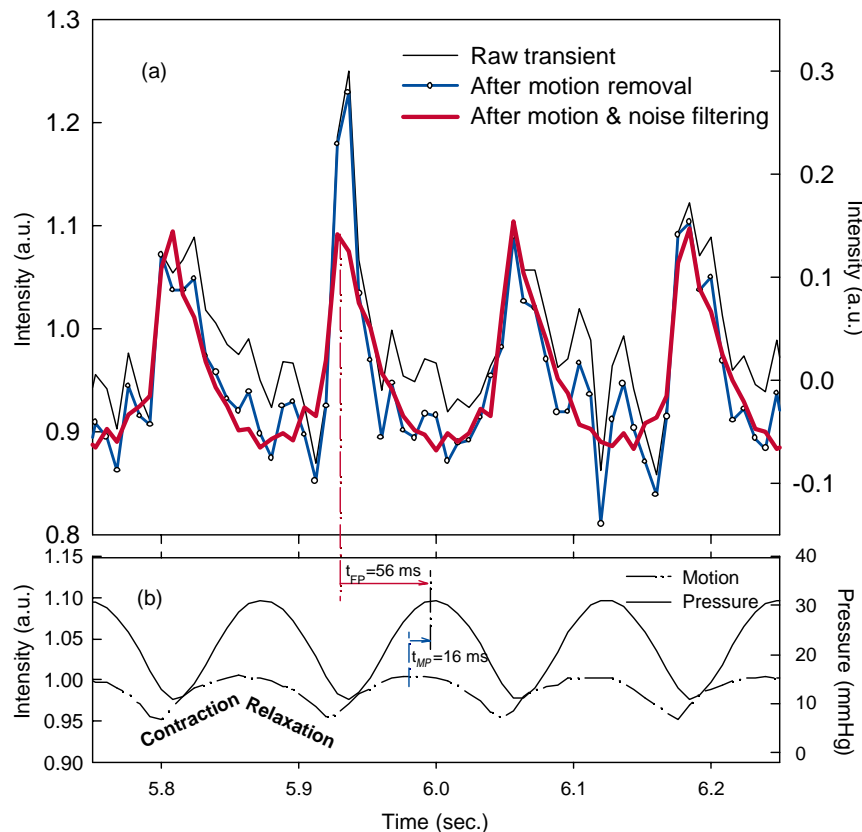

Fig. 6. (a) Comparison of raw transient data (*light solid line*) with results after motion removal (*circled solid line*) and a further noise filtering process (*thick solid line*). (b) Corresponding left ventricular pressure signal (*solid line*) with motion waveform (*dotted dashed line*) obtained simultaneously from the mouse heart. The percentage of motion in the transient signal is estimated by using $(\text{Motion}_{peak} - \text{Motion}_{base})/(\text{Transient}_{peak} - \text{Transient}_{base})$ which equals 22.9%. The latency of pressure waveform to the transient (t_{FP}) is 56 ms and to the motion wave (t_{MP}) is 16 ms.

the reference. Thus, this subtraction process adds the square root of two times the noise of the individual spectrum on the processed spectrum.

To reduce this unwanted random noise, filtering using multiple bandpass filters centralized at harmonic frequencies of 8 Hz was applied to the spectra of transients. The transmittance of the filters $\phi(\omega)$ to be 1 or 0 was determined according to the model described above in Eq. (9). Empirically, we consider the transmittance to be switched to 1 when PSD was 10-fold greater than the average noise spectral level ($\sim$1, as shown in Fig. 5b). Fig. 5c shows the digital filtering of the multiple bandpass filters for the data. For comparison, the PSD of transients before and after bandpass filtering are shown in Fig. 5d, illustrating the removal of random noise in the frequency domain through these multiple filters.

Fig. 5e displays the effect of Kernel low-pass filtering applied to reduce the influence of the high frequency noise on the signal. The bandwidth of the filter is $\sim$33 Hz. The envelope of PSD drops a little over 30 Hz after this processing, thus cutting off the influence of high frequency noise on the transient signal, as shown in Fig. 5f.

The data are then back-transformed to the time domain after these processes. Fig. 6a shows the comparison of the raw transient data (light solid line) with the results after motion removal (circled solid line) and after further noise filtering (thick solid line). This indicates that the process of subtracting motion from data in the frequency power spec-

trum removes the additional increase in fluorescence intensity due to a closer position of the heart surface with respect to the optical detector caused by cardiac contraction. However, this stage does not help to eliminate the influence of noise on the data. For instance, the abnormal sharp peak in the second transient trace shown in Fig. 6a has not improved after this subtraction process. As expected, the multiple bandpass and Kernel low-pass filters play an important role in the noise elimination, as illustrated in the transient traces after the processes in Fig. 6a. The processed results show that the upstroke portion of the transients is consistent with the data before processing, thus indicating that this method does not interfere with the high frequency components of the transients.

4.3. Time-shift independence of motion wave obtained in reference

Based on the theoretical model described above, the accuracy of data processing should not be affected by a varying time dependence of the heart motion signal obtained by the reference channel. To test this, two experimental data with similar amplitude of motion are selected. As described in the figure legends of Figs. 6 and 7, the motion amplitudes of these two experiments with respect to the corresponding transients are 22.9 and 21.8%, respectively. In addition, the latency of pressure waveform to the calcium transient (t_{FP})
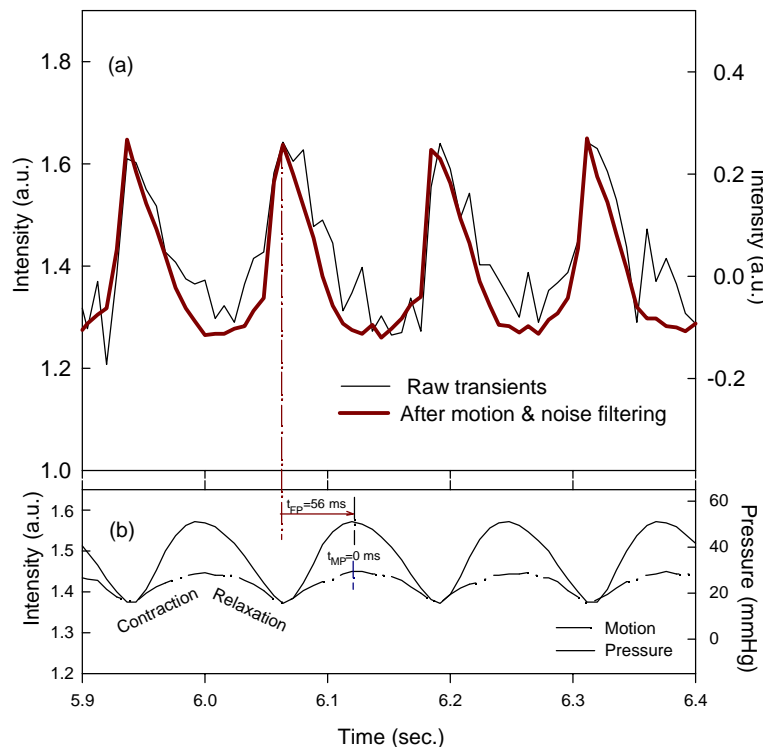

Fig. 7. (a) Comparison of the raw transient data (*light line*) and the resulting transient after motion removal and noise filtering (*thick line*). (b) The corresponding left ventricular pressure signal (*solid line*) with motion waveform (*dotted dashed line*) obtained simultaneously from the mouse heart. The percentage of motion in the transient signal is 21.8%. The latency of pressure waveform to the transient t_{FP} is 56 ms and there is no latency between the pressure and motion waves (i.e. $t_{MP} = 0$).

is identical (~56 ms) in both cases. However, the timing of the motion waveform relative to the pressure waveform, i.e. t_{MP}, is different for these two examples: Fig. 6b is 16 ms, and Fig. 7b is zero. As t_{FP} is similar in both examples, we assume that cardiac function is similar in both cases. Thus, the difference of the time phase of the motion wave in these two experiments indicates an inaccurate time-phase delay in one of these experiments, detected by the reflectance channel. We expect this lag artifact of reference will not influence the accuracy of motion correction using the methodology presented. The processed results of these two experimental transients are shown in Figs. 6a and 7a. The clear transient shape overlaps with the raw transients in both results and demonstrates that the processing is independent of the time phase of the motion wave obtained by the reference.

4.4. Comparison of the processed calcium transient signal with calcium transients from an immobilized heart

Transient signals with significant motion and minimal motion artifact detected simultaneously from the freely moving portion and immobilized area of the heart are shown in Fig. 8a, indicating a dramatic difference between the signals with significant (light solid line) and minimal motion (circled solid light) artifacts. To evaluate our processing accuracy, we plot the transients after processing in the same figure. As can be seen, the transients recovered from the high motion case are very similar to the transients with minimal motion artifact, thus validating the method.

The impact of this processing method on removing motion can be estimated by comparing the value of the residual motion artifact/noise before and after processing of the transients to the measurement simultaneously obtained from the heart with minimal motion artifact. As shown in Fig. 8b, at the part of the cardiac cycle approximately where the motion was the largest (i.e. ~50% recovery time) the fluctuation in fluorescence with respect to transient dynamic (from base to peak) decreases from $20 \pm 2\%$ (before processing) to $5 \pm 1\%$ (after processing), demonstrating a fourfold decrease in the motion artifact.

The consistency of the transients has been examined by analyzing the differentials of 78 transient cycles obtained consecutively from a heart in ~10 s correspondingly to those detected with minimum motion. The average differential in the fluorescence intensity decreased from 0.037 ± 0.002 (before processing) to 0.016 ± 0.001 (after processing),
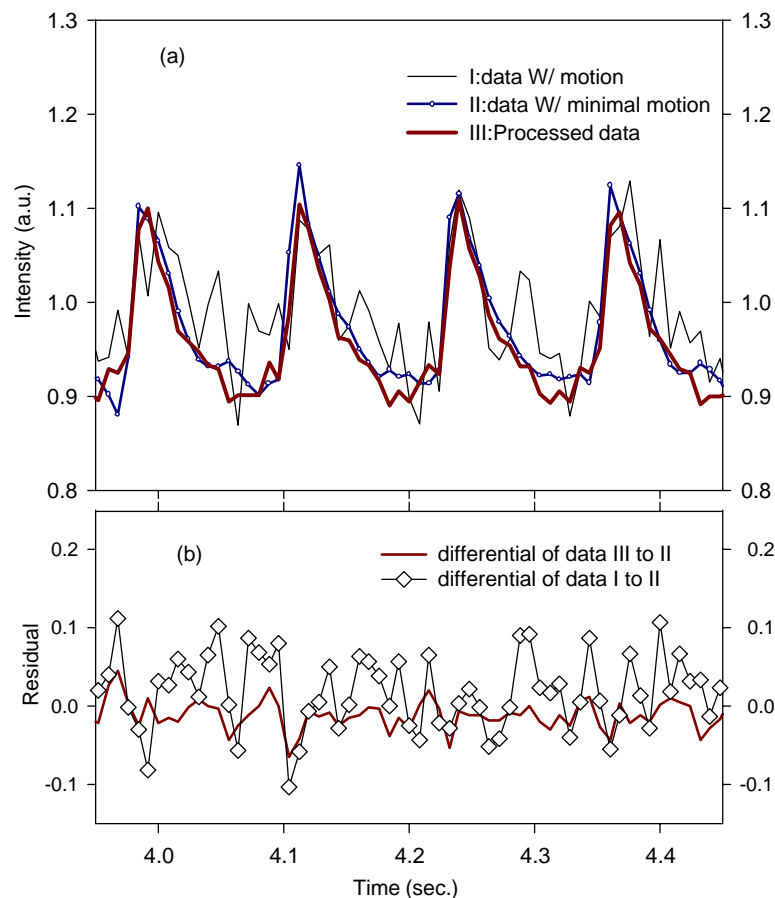

Fig. 8. (a) Comparison of the raw transient signal (I: *light solid line*) with the processed signal from a freely moving heart (III: *thick solid line*), and the signal from an immobilized surface of the heart (II: *circled solid line*). (b) Comparison of the deviations of the raw transient data (*diamonds*) and data after processing (*solid line*) to the measurement with minimal motion.

indicating a much improved periodicity of the transients as a function of time.

5. Discussion

Motion artifact is a substantial problem in imaging and spectroscopic measurements, particularly in a living tissue or isolated organ, such as muscle or heart, in which contraction occurs. Previous investigators have attempted to suppress motion artifacts in the measurements of fluorescence spectroscopy of perfused hearts, using the following methods: (1) physical restriction of the heart to limit its motion with respect to the light detectors [5–7]; (2) using reflected light as a reference to ratio [13] or subtract [10] from the fluorescence signal; or (3) using a fluorescence standard [2] or ligand-insensitive emission wavelength [9] as the reference signal to correct for motion. With these techniques, motion artifact intensity can be significantly reduced. However, each of these has limitations. For instance, method 1 can cause partial tissue ischemia [5,6]; method 2 cannot accurately correct signal from motion artifact in the case of a mismatched time dependence of the motion signal; and method 3 is only limited to those fluorescence dyes with a spectral shift upon binding calcium and a small wavelength difference between the reference and signal [11,19]. Comparing these three methods, reflectance as a reference can be used for any fluorescence measurement using either ratiometric (e.g. Indo-1) or non-ratiometric (e.g. Rhod-2) dyes. It is convenient for most fluorescence applications, and has potential for applications in vivo. Therefore, our goal was to improve the procedures for using reflected excitation light as a reference in fluorescence spectroscopy and imaging.

In this study, we present a frequency filtering technique to eliminate the influence of the periodic perturbation of motion and detection noise on fluorescence spectroscopy. The removal of motion artifact is preformed by subtracting the power spectrum of the normalized motion wave from that of the fluorescence transients in the frequency domain. There are two advantages of the frequency domain technique. First, it is independent of any time differences of the motion signal with respect to motion effects on the fluorescence signal due to the phase insensitivity of the magnitude calculation of the spectral power densities. This feature was tested by analyzing experimental transients from the perfused mouse heart with the same time latency (t_{FP}) of peak pressure to the fluorescence calcium transient peak, but a different time difference from the motion waveform to peak pressure as illustrated in Figs. 6 and 7. The results demonstrate the independence of the motion correction method to the time-phase shift artifact of the reference.

The second advantage of working in the frequency domain is that filtering of the transient data can be performed by using multiple digital bandpass filters that can minimize noise. To suppress high frequency noise, the Kernel method was used [20]. The cut off frequency of the Kernel filter was determined based on the highest frequency component detected in the transient signal. In addition, notch filters were placed around the frequencies that contained significant spectral density. With the combination of these filters, a significant improvement in SNR was achieved. The back-transformed time traces of calcium transients with a clearly rapid upstroke during systole and a gradual decline during diastole in a cardiac cycle demonstrates the efficiency of the process.

A key to the successful implementation was to make sure the gains of the reflected excitation and fluorescence matched. This was accomplished by calibrating the gains on the heart before loading Rhod-2. The fact that the frequency domain power spectral densities scaled very well indicates that this calibration was effective. Indeed, it should be possible to do the gain correction in the frequency domain after loading Rhod-2 by matching the noise intensities of the reflected light and fluorescence.

To examine the methodology proposed here, we have used hearts perfused with perfusate calcium 1.5 mM which typically results in developed pressures of approximately 25 mmHg. This is lower than the developed pressures that we see at the more frequently used perfusate calcium of 2.5 mmHg (55–65 mmHg), we used the low calcium perfusate because this is a condition where the data provide large motion and relatively low signal to noise due to low calcium suitable for a test of the data analysis.

Any filtering process affects the time domain characteristics. The low-pass Kernel filter decreases the very high frequency components and the notch filter can change the frequency domain shape. The gain in reducing motion and improving signal to noise at this stage offsets the potential alterations in the fluorescence waveform due to the filtering. To minimize the distortion of the discrete measurement data to approach the continuous signals, such as fluorescence transients, we sampled at a rate sufficiently rapid to give 16 points per cardiac cycle and ~4 points over the upstroke period of the transient where the highest frequency presents. In discrete Fourier transform, we use 1024 consecutive sampled data that cover sufficient cardiac cycles (e.g. 64 cycles) to minimize the limits caused by loss of resolution in frequency, thus optimizing the transfer precision. The processed transients acquired with excessive motion artifact and noise were compared with transients with minimal motion, which were acquired simultaneously from the same heart, and obtained by immobilizing the heart against the detection optical window. The small residuals between the post-processed signal compared to the transients with minimal motion (see Fig. 8b) demonstrate consistency of the processed signal with the physical measurement, thus validating this technique.

In conclusion, the frequency domain filtering method can be used to effectively isolate calcium fluorescence transients from fluctuations due to motion. This may prove useful when applying optical techniques to in vivo and clinical studies, especially those studies with time varying signals, such as calcium transients.

Appendix A

A.1. Simplification of reflectance spectroscopy

Similar to the expression of Eq. (1), the reflectance intensity measured at excitation wavelength can be described as,

$$S_{ex}(t) = H_{ex}[E_{em}(t) + B_{ex}(t) + I_{ex}(t)] \quad (A.1)$$

where H_{ex} is the gain of reference channel, $E_{em}(t)$ is the stray fluorescence emission from the heart, $B_{ex}(t)$ is the tissue background emission, and $I_{ex}(t)$ is the intensity of the reflected excitation light.

As the stray light of the fluorescence intensity, i.e. $E_{em}(t)$ in Eq. (A.1) is much lower than the reflectance of background and excitation light, i.e. $E_{em}(t) \ll B_{ex}(t) + I_{ex}(t)$. Thus, it can be negligible, so, the above Eq. (A.1) can be simplified into

$$S_{ex}(t) \approx H_{ex}[B_{ex}(t) + I_{ex}(t)] \quad (A.2)$$

A.2. Derivation of relationship between the intensities of emission to excitation at baseline and the gain of the corresponding channels

The average intensities of emission $\overline{S_{em}^0}$ and excitation $\overline{S_{ex}^0}$ at baseline prior to loading fluorescence dye can be expressed as

$$\overline{S_{em}^0} = H_{em} \frac{\int_0^{t_{max}}[B_{em}(t) + I_{ex}(t)]dt}{\int_0^{t_{max}}dt}$$

$$= \frac{H_{em}}{t_{max}} \int_0^{t_{max}}[B_{em}(t) + I_{ex}(t)]dt \quad (A.3)$$

$$\overline{S_{ex}^0} = H_{ex} \frac{\int_0^{t_{max}}[B_{ex}(t) + I_{ex}(t)]dt}{\int_0^{t_{max}}dt}$$

$$= \frac{H_{ex}}{t_{max}} \int_0^{t_{max}}[B_{ex}(t) + I_{ex}(t)]dt \quad (A.4)$$

where time interval from 0 to t_{max} represents the time period of the data acquisition of emission and excitation from the

tissue at baseline prior to loading the fluorescence dye. Our previous experimental finding shows that the autofluorescence intensity does not change much at excitation (524 nm) and emission (589 nm) wavelengths [6], i.e. $B_{ex} \approx B_{em}$. When taking ratio of Eqs. (A.3) and (A.4), we can have

$$\frac{\overline{S_{em}^0}}{\overline{S_{ex}^0}} \approx \frac{H_{em}}{H_{ex}} \quad (A.5)$$

A.3. Power spectrum density of fluorescence and reflectance reference

By definition, the magnitude-mode frequency domain spectrum of a signal is the squared magnitude of its Fourier transform [18]. It can be derived by calculating the Fourier transform of the autocorrelation function, i.e. the correlation of a signal with itself. For instance, the autocorrelation of the above fluorescence emission S_{em}, denoted as Corr(S_{em}, S_{em}) below, can be expressed as

$$\text{Corr}(S_{em}, S_{em}) = \int_{-\infty}^{+\infty} S_{em}(\tau + t)S_{em}(\tau)d\tau$$

$$= \frac{1}{2\pi} \int_{-\infty}^{+\infty} |S_{em}(\omega)|^2 e^{i\omega t}\, d\omega \quad (A.6)$$

where $|S_{em}|^2$ is the magnitude-mode spectrum in frequency domain that is ordinarily referred to as the PSD of S_{em}.

Substituting Eq. (1) into the right-hand side of Eq. (A.6) gives

$$\frac{1}{2\pi} \int_{-\infty}^{+\infty} |H_{em}[E_{em}(\omega) + B_{em}(\omega) + I_{ex}(\omega)]|^2 e^{i\omega t}\, d\omega$$

$$\approx \frac{1}{2\pi} \int_{-\infty}^{+\infty} H_{em}^2[|E_{em}(\omega)|^2 + |B_{em}(\omega)|^2$$

$$+ ||I_{ex}(\omega)|^2|]e^{i\omega t}\, d\omega \quad (A.7)$$

Practically, the signal of the fluorescence E_{em}, background emission B_{em}, and the scattered residual excitation light I_{ex} are uncorrelated. Their cross product, when integrated over frequency ω, gives zero, thus are ignored in Eq. (A.7). Therefore, $|S_{em}(\omega)|^2$ can be expressed as

$$|S_{em}(\omega)|^2 \approx H_{em}^2\{|E_{em}(\omega)|^2 + |B_{em}(\omega)|^2 + |I_{ex}(\omega)|^2\} \quad (A.8)$$

Similarly, the PSD function for the normalized reference $|S_{ex}^{normalized}(\omega)|^2$ can be expressed as

$$|S_{ex}^{normalized}(\omega)|^2 \approx H_{em}^2\{|B_{ex}(\omega)|^2 + |I_{ex}(\omega)|^2\} \quad (A.9)$$

A.4. Weight function to filter random noise in power density spectrum

As described in Eq. (8), the detected fluorescence signal $E_{em}(\omega)$ consists of noiseless signal $E'_{em}(\omega)$ and noise item $N(\omega)$, i.e.

$$E_{em}(\omega) = E'_{em}(\omega) + N(\omega) \quad (A.10)$$

To eliminate the influence of noise on the power density spectrum of the signal, our task is to make the corrupted signal $E_{em}(\omega)$ close to the uncorrupted signal $E'_{em}(\omega)$ after the filtering process using the weight function of $\phi(\omega)$ in the frequency domain, which can be explained as

$$|E'_{em}(\omega)|^2 \approx \phi(\omega)|E_{em}(\omega)|^2 \approx \phi(\omega)|E'_{em}(\omega) + N(\omega)|^2$$

(A.11)

As described in Section 2, the noise waveform is random as a function of the frequency. It is independent of signal strength which makes the correlation of $E'_{em}(\omega)$ and $N(\omega)$ to be zero. Therefore, Eq. (A.11) can be approximated as

$$|E'_{em}(\omega)|^2 \approx \phi(\omega)\{|E'_{em}(\omega)|^2 + |N(\omega)|^2\} \qquad (A.12)$$

Then, $\phi(\omega)$ can be expressed as

$$\phi(\omega) = \frac{|E'_{em}(\omega)|^2}{|E'_{em}(\omega)|^2 + |N(\omega)|^2} \qquad (A.13)$$

It can be simplified under the following conditions,

$$\begin{cases} \phi(\omega) = \dfrac{|E'_{em}(\omega)|^2}{|E'_{em}(\omega)|^2 + |N(\omega)|^2} \to 1, & \text{for } |E'_{em}(\omega)| \gg |N(\omega)| \\[2ex] \phi(\omega) = \dfrac{|E'_{em}(\omega)|^2}{|E'_{em}(\omega)|^2 + |N(\omega)|^2} \to 0, & \text{for } |E'_{em}(\omega)| \ll |N(\omega)| \end{cases}$$

(A.14)

which means that $\phi(\omega)$ should be equal to 1 (no filtering) at the frequencies where the signal predominates, but zero (completely filtered) at the frequencies where noise predominates.

References

[1] D.G. Allen, J.R. Blinks, The interpretation of light signals from aequorin-injected skeletal and cardiac cells: a new method of calibration, in: C.A. Christophersheley, A.K. Campbell (Eds.), Detection and Measurement of Free Ca^{2+} in Cells, Elsevier, New York, Oxford, 1979.

[2] A.P. Koretsky, L.A. Katz, R.S. Balaban, Determination of pyridine nucleotide fluorescence from the perfused heart using an internal standard, Heart Circ. Physiol. 22 (1987) H856–H980.

[3] R.V. Brandes, M. Figueredo, S.A. Camacho, M.W. Weiner, Ca^{2+} measurements in perfused hearts by fluorescence. Effects of motion, tissue absorbance and NADH, Circulation 84 (Suppl. II) (1991) II-402.

[4] M.L. Field, A. Azzawi, P. Styles, C. Henderson, A.M. Seymour, G.K. Radda, Intracellular Ca^{2+} transients in isolated perfused rat heart: measurement using the fluorescent indicator Fura-2/AM, Cell Calcium 16 (2) (1994) 87–100.

[5] P.J. del Nido, P. Glynn, P. Buenaventura, G. Salama, A.P. Koretsky, Fluorescence measurement of calcium transients in perfused rabbit heart using Rhod-2, Am. J. Physiol. 274 (1998) H728–H741.

[6] C. Du, G.A. MacGowan, D.L. Farkas, A.P. Koretsky, Calcium measurement in perfused mouse heart: quantitating fluorescence and absorbance of Rhod-2 by application of photon migration theory, Biophys. J. 80 (2000) 549–561.

[7] G.A. MacGowan, C. Du, A.P. Koretsky, D.L. Farkas, Rhod-2 based measurements of intracellular calcium in the perfused mouse heart: cellular and subcellular localization, and response to positive inotropy, J. Biomed. Opt. 6 (2001) 23–30.

[8] B. Sato, A. Tanaka, S. Mori, N. Yanabu, T. Kitai, A. Tokuka, T. Inomo, S. Iwata, Y. Yamaoka, B. Chance, Quantitative analysis of redox gradient within the rat liver acini by fluorescence images: effects of gluocagon perfusion, Biochim. Biophys. Acta 1268 (1995) 20–26.

[9] R. Brandes, V.M. Figueredo, S.A. Camacho, B.M. Massie, M.W. Weiner, Suppression of motion artifacts in fluorescence spectroscopy of perfused hearts, Am. J. Physiol. 263 (1992) H972–H980.

[10] M. Osbakken, A. Mayevsky, I. Ponomarenko, D. Zhang, C. Duska, B. Chance, Combined in vivo NADH fluorescence and ^{31}P NMR to evaluate myocardial oxidative phosphorylation, J. Appl. Cardiol. 4 (1989) 305–313.

[11] R.P. Haugland, M.Z. Spence, L.D. Johnson, Handbook of Fluorescent Probes and Research Chemicals, 6th ed., Molecular Probes Inc., 1996, pp. 511–514.

[12] R.S. Kramer, R.D. Pearlstein, Cerebral cortical microfluorometry at isosbestic wavelengths for correction of vascular artifact, Science 205 (1979) 693–696.

[13] G. Renault, E. Raynal, M. Sinet, M. Muffat-Joly, J.P. Berthier, J. Cornillault, B. Godard, J.J. Pocidalo, In situ double-beam NADH laser fluorimetry: choice of a reference wavelength, Am. J. Physiol. 245 (Heart Circ. Physiol. 15) (1984) H491–H499.

[14] I.R. Wendt, J.B. Chapman, Fluorometric studies of recovery metabolism of rat fast- and slow-twitch muscles, Am. J. Physiol. 230 (1976) 1644–1649.

[15] B.C. Smith, Fundamental of Fourier Transform Infrared Spectroscopy, CRC, Florida, 1996.

[16] A.G. Marshall, F.R. Verdun, Fourier Transforms in NMR, Optical and Mass spectrometry: A User's Handbook, Elsevier, New York, 1990.

[17] C.W. Frank, J.L. Koenig, E.D. MeerWall, S.N. Semerak, Spectroscopy: NMR, Fluorescence, FT-IR. Springer-Verlag, Berlin, Heidelberg, New York, Tokyo, 1984.

[18] T.M. Peters, J. Williams (Eds.), The Fourier Transform in Biomedical Engineering, Birkhauser, Boston, 1998.

[19] W.L. Butler, Absorption spectroscopy of biological materials, Methods Enzymol. 24 (1972) 3–25.

[20] W. Yu, G. Sommer, Daniilidis, 3D-Orientation signatures with conic kernel filtering for multiple motion analysis, IEEE Computer Vision and Pattern Recognition 1 (2001) I-299–I-306.

[21] Y.W. Qian, W.T. Clusin, S.F. Lin, J. Han, R.J. Sung, Spatial heterogeneity of calcium transient alternans during the early phase of myocardial ischemia in the blood-perfused rabbit heart, Circulation 104 (2001) 2082–2087.

[22] B.R. Choi, G. Salama, Simultaneous maps of optical action potentials and calcium transients in guinea-pig hearts: mechanisms underlying concordant alternans, J. Physiol. 529.1 (2000) 171–188.

[23] G.A. MacGowan, C. Du, D.F. Weiczorek, A.P. Koretsky, Compensatory changes in Ca^{2+} and myocardial O_2 consumption in β-tropomyosin transgenic hearts, Am J. Physiol. Heart Circ. Physiol. 281 (2001) H2539–H2548.

[24] C. Du, G.A. Macgowan, D.L. Farkas, A.P. Koretsky, Calibration of the calcium dissociation constant of Rhod-2 in the perfused mouse heart using manganese quenching, Cell Calcium 29 (2001) 217–227.